Title
HNRNPA2B1 Is a Mediator of m6A-Dependent Nuclear RNA Processing Events

Authors
Alarcón, Claudio R
Goodarzi, Hani
Lee, Hyeseung
et al.

Peer reviewed

HNRNPA2B1 is a mediator of m6A-dependent nuclear RNA processing events

Claudio R. Alarcón[1], **Hani Goodarzi**[1,3], **Hyeseung Lee**[1,3], **Xuhang Liu**[1], **Saeed Tavazoie**[2], and **Sohail F. Tavazoie**[1,*]

[1]Laboratory of Systems Cancer Biology, Rockefeller University

[2]Department of Biochemistry and Molecular Biophysics, and Department of Systems Biology, Columbia University

SUMMARY

N^6-methyladenosine (m6A) is the most abundant internal modification of messenger RNA. While the presence of m6A on transcripts can impact alternative splicing, a nuclear reader of this mark that mediates the processing of nuclear transcripts has not been identified. We find that the RNA-binding HNRNPA2B1 protein binds m6A-bearing RNAs *in vivo* and *in vitro* and its biochemical footprint matches the m^6A consensus motif. HNRNPA2B1 directly binds a set of nuclear transcripts and modulates their alternative splicing in a similar manner as the m^6A 'writer' METTL3. Moreover, HNRNPA2B1 binds to m^6A marks in a subset of primary-miRNA transcripts, interacts with the microRNA Microprocessor complex protein DGCR8, and promotes primary miRNA processing—phenocopying the effect of METTL3 depletion on the processing of these precursor transcripts. We propose HNRNPA2B1 to be a nuclear reader of the m^6A mark and to mediate, in part, this mark's effects on primary microRNA processing and alternative splicing.

INTRODUCTION

Nucleotide modifications can expand the information content of nucleic acids. Methylation of cytosines on promoter DNA, for example, can alter the transcriptional output of genes. RNA can also be modified by a myriad of marks and mRNA modifications including among others *N6*-methyladenosine, 5-methylcytosine, 2n *O*-methylation of ribose and pseudouridylation (Jaffrey, 2014). The functional roles of the majority of these chemical modifications are unknown. The most common internal modification of eukaryotic messenger RNA is methylation of the N^6 nitrogen on adenosine referred to as N^6-methyladenosine (m6A). Each transcript contains 1–3 m^6A marks on average, which are located in specific positions in introns, exons, and untranslated regions. Methylation of specific positions is non-stoichiometric with only a fraction of transcripts containing this mark at specific sites. While this important modification was discovered over four decades

*Corresponding author: Sohail Tavazoie, Leon Hess Associate Professor, Head, Laboratory of Systems Cancer Biology, Rockefeller University, Box 16, 1230 York Avenue, New York, NY 10065 USA, Phone: 212-327-7208, Fax: 212-327-7209, stavazoie@mail.rockefeller.edu.
[3]These authors contributed equally to this work

ago, the transcriptome-wide mapping of this mark using next-generation sequencing analysis has recently revived interest in the biological role(s) of m^{6}A (Dominissini et al., 2012; Goodarzi et al., 2012; Meyer et al., 2012; Wang et al., 2014a).

Methyltransferase like 3 (METTL3) was the first methyltransferase implicated in placing m^{6}A on RNA (Dominissini et al., 2012; Meyer et al., 2012; Wei and Moss, 1974). METTL14, which exists in complex with METTL3, has also been shown to exhibit m^{6}A methyltransferase activity (Liu et al., 2014). Fat mass and obesity-associated protein (FTO) was recently identified as an enzyme that can remove this mark (Jia et al., 2011). Classical experiments suggested a role for m^{6}A in the nuclear processing of viral and non-viral transcripts (Carroll et al., 1990; Katz et al., 2015; Liu et al., 2015; Stoltzfus and Dane, 1982). More recent molecular studies have demonstrated m^{6}A to exhibit both a nuclear role in splicing (Dominissini et al., 2012) and a cytoplasmic role in the regulation of RNA stability (Batista et al., 2014; Wang et al., 2014a). We have recently found that m^{6}A plays an additional role in the nucleus in controlling microRNA biogenesis. M^{6}A was found to be enriched in primary microRNA transcripts. Reducing m^{6}A levels by depleting the m^{6}A writer METTL3 reduced the levels of the majority of expressed microRNAs (Alarcon et al., 2015). This effect occurred in the nucleus since METTL3/m^{6}A depletion reduced the association of the DGCR8-containing microRNA processing complex with primary microRNAs and caused unprocessed primary microRNA precursors to accumulate in the nucleus. These findings are consistent with a model wherein the m^{6}A RNA mark is recognized and bound by a nuclear reader protein, which recruits the DGCR8 Microprocessor complex to pri-miRNA containing transcripts resulting in their processing. Recently the YTH domain family 2 (YTHDF2) protein was identified as a 'reader' of m^{6}A and found to regulate the stability of m^{6}A-bearing transcripts in the cytoplasm (Wang et al., 2014a). The proposed role of m^{6}A in the control of alternative splicing and our recent findings regarding its impact on primary microRNA processing (Alarcon et al, 2015), suggest the existence of nuclear reader(s) of m^{6}A that bind this mark and mediate nuclear processing events that are mechanistically distinct from RNA stability regulatory events that could occur in the cytoplasm.

We herein identify HNRNPA2B1 as a nuclear reader of m^{6}A. HNRNPA2B1 binds to RGm^{6}AC containing sites on nuclear RNAs *in vivo* and *in vitro*. HNRNPA2B1 regulates the alternative splicing of exons in a set of transcripts in a similar manner as METTL3, the m^{6}A 'writer'. The global impact of HNRNPA2B1 depletion on alternative splicing is highly correlated with the global effect of METTL3 depletion on alternative splicing. HNRNPA2B1 depletion also impairs the nuclear processing of a subset of microRNAs whose maturation is dependent on METTL3 activity. Moreover, HNRNPA2B1 interacts with the DGCR8 protein, a component of the pri-miRNA Microprocessor complex and facilitates the processing of pri-miRNAs. Our findings implicate HNRNPA2B1 as a nuclear reader and effector of the m^{6}A mark.

RESULTS

HNRNPA2B1 binds to m⁶A-bearing sites in the transcriptome

The presence of the m^6A mark has been historically associated with the processing of nuclear transcripts. Our identification of m^6A as a regulatory mark that promotes the processing of pri-microRNA transcripts a process that occurs in the nucleus suggested the existence of one or more nuclear readers of this mark that mediate its downstream effector functions. Several approaches that combine UV cross-linking of RNA-binding proteins with immunoprecipitation and deep-sequencing of bound RNAs have proven powerful at mapping the sites of interaction between RNA-binding proteins and their target RNAs (Hafner et al., 2010; Konig et al., 2010; Ule et al., 2005). Our laboratories have in the past few years conducted a number of such high-throughput sequencing of RNA isolated by crosslinking immunoprecipitation (HITS-CLIP; Zhang and Darnell, 2011) studies to map the genome-wide binding of a variety of RNA-binding proteins. Our analysis of the direct binding sites of one such RNA-binding protein, HNRNPA2B1 (Goodarzi et al., 2012), suggested that it might act as a reader of the m^6A mark. HNRNPA2B1 is a member of the hnRNP family of RNA-binding proteins that are known to associate with pre-mRNAs in the nucleus. The m^6A mark is known to occur within the RG<u>A</u>C motif, with R representing a purine (Schibler et al., 1977). To test the possibility that HNRNPA2B1 also recognizes this motif, we assessed the abundance of this sequence among the HNRNPA2B1 HITS-CLIP peaks relative to randomly generated sequence counterparts with similar dinucleotide frequencies (Giannopoulou and Elemento, 2011). Indeed, using the FIRE analysis pipeline (Elemento et al., 2007), we observed a highly significant enrichment of the RGAC element in HNRNPA2B1 binding sites (Figure 1A).

We next overlapped the m^6A peaks from an RNA-seq analysis of m^6A-immunoprecipitated nuclear RNA (m6A-seq; Alarcon et al., 2015) with HNRNPA2B1 binding peaks obtained from HITS-CLIP of endogenous nuclear HNRNPA2B1 performed for this study in MDA-MB-231 breast cancer cells. We noted a significant number of cases wherein the HNRNPA2B1 peaks overlapped with m^6A peaks (Figure 1B, S1A; *p*-value< 1E-3), consistent with an enrichment of m^6A at HNRNPA2B1 binding sites. Of the 1912 human genes bound by HNRNPA2B1 and containing m^6A peaks, 426 contained RGAC instances overlapping both an HNRNPA2B1 HITS-CLIP peak and an m^6A-seq peak (FDR<10%). Conducting this analysis on HITS-CLIP data we had previously generated for MBNL1 and TARBP2 revealed zero such cases of overlap for these RNA-binding proteins.

The enrichment of the RGAC motif in HNRNPA2B1 binding sites may be due to general proximity of the RGAC motif to the HNRNPA2B1 binding sites rather than due to direct interactions with the RGAC motif. The RNA-binding protein hnRNPC, for example, has been shown to bind near rather than directly to the RGAC motif. Thus, to study the specificity of overlap between the HNRNPA2B1 footprint and the m^6A consensus motif at nucleotide resolution, we took advantage of cross-linking induced deletions that are a hallmark of HITS-CLIP experiments and which provide a nucleotide-level map of physical points of interaction (Zhang and Darnell, 2011). For this, we limited our search to the cross-linking induced deletions that mark the sites of direct interactions between HNRNPA2B1

and its target RNAs (CIMS; Zhang and Darnell, 2011). We also defined a set of control sequences consisting of deletion-containing reads that represent the background occurrence of deletion events during HITS-CLIP sample preparation (i.e. these reads were not part of a peak or cluster; Figure S1). We then used FIRE to re-evaluate the abundance of the RGAC motif in HNRNPA2B1 footprints (i.e. crosslinking-induced deletion sites along with 5nt flanking sequences on either side). We observed a highly significant enrichment of RGAC motifs at these cross-linking induced deletions (p-value <10E-26, z-score=109; Figure 1C). A similar analysis applied to two other RNA-binding proteins for which comparable HITS-CLIP data was available revealed HNRNPA2B1 to be unique among this group in exhibiting a significant enrichment for proximal binding to the RGAC motif (Figure 1C and S1C). Importantly, 6.8% of the nuclear HNRNPA2B1 cross-linking induced deletions overlapped with an m^6A peak; whereas, only 0.34% of the background deletions overlapped with m^6A sites (20-fold enrichment, Figure S1D). These findings strongly support a role for HNRNPA2B1 in directly binding to a subset of m^6A consensus sequences within the transcriptome.

METTL3 and HNRNPA2B1 regulate common alternative splicing events

The m^6A mark has been associated with (Carroll et al., 1990; Katz et al., 2015; Stoltzfus and Dane, 1982) and causally implicated in pre-mRNA processing (Dominissini et al., 2012). Depletion of METTL3 has also been shown to impact alternative splicing (Dominissini et al., 2012). We hypothesized that HNRNPA2B1, by acting downstream of m^6A placement by METTL3, may impact alternative splicing in a similar manner as METTL3. If this were the case, depleting HNRNPA2B1 should result in similar alterations in alternative splicing patterns as depletion of METTL3. To test this, we conducted high-throughput RNA-sequencing (RNA-seq) on nuclear RNA from cells depleted of METTL3 and those depleted of HNRNPA2B1. We then employed MISO, a probabilistic framework (Katz et al., 2010), to quantify the relative expression of alternatively spliced exons in METTL3 and HNRNPA2B1 knockdown cells as well as controls. The differences in MISO-calculated Ψ (psi, percent-spliced in) values between each of the knockdown samples and the control samples were used as a measure of modulations in alternative splicing events upon depletion of each of these factors. Consistent with a role for HNRNPA2B1 in mediating alternative splicing effects downstream of METTL3/m^6A, we observed that the global impact on alternative splicing was highly correlated in cells depleted for each of these genes. This effect was observed in skipped exons (ρ= 0.335; $p<10^{-200}$; Figure 2A), retained introns (ρ= 0.373; $p<10^{-140}$; Figure 2B), alternative first exons (ρ= 0.378; $p<10^{-300}$; Figure 2C) and alternative last exons (ρ= 0.299; $p<10^{-170}$; Figure 2D). The effects on alternative splicing in the context of HNRNPA2B1 and METTL3 depletion were seen in two independent cell lines (Figure 2E–F and Figure S2.). These findings reveal that HNRNPA2B1 depletion has similar genome-wide consequences on alternative splicing as METTL3 depletion. These observations along with our findings that HNRNPA2B1 binds m^6A sites support a model whereby HNRNPA2B1 would mediate, in part, the alternative splicing effects of METTL3 and the m^6A mark.

HNRNPA2B1 promotes processing of METTL3-dependent microRNAs and interacts with the Microprocessor machinery

We next asked whether HNRNPA2B1 governs the processing of pri-miRNAs that are dependent on METTL3/m[6]A for their processing. For this, we performed global microRNA profiling in HEK293 cells depleted of HNRNPA2B1. HNRNPA2B1 knockdown caused a reduction in the levels of a large number of microRNAs (Figure 3A and Figure S3). This reduction could also be visualized as a left-shift in the population-level expression of miRNAs (Figure 3B; p<1e-3). The reduction in mature microRNA expression mirrored what was previously observed upon METTL3 depletion (Alarcon et al., 2015).

We next investigated the overlap between the set of miRNAs impacted by HNRNPA2B1 depletion and those impacted by METTL3 depletion. Importantly, 95% (58 out of 61) of the miRNAs whose levels decreased by more than 50% when HNRNPA2B1 was depleted were also affected, with similar intensity, upon depletion of METTL3 (p<1e-24, Figure 3C and Table S1). The fraction of miRNAs affected by HNRNPA2B1 depletion was roughly half of the total miRNAs regulated by METTL3 indicating that HNRNPA2B1 regulates a major subset, but not all, of the m[6]A dependent miRNAs.

In order to validate these findings using an independent approach, we performed quantitative PCR (qPCR) for specific miRNAs in the setting of HNRNPA2B1 knockdown using additional cell lines. Consistent with the findings described above, HNRNPA2B1 depletion caused a significant reduction in the expression levels of the mature forms of a number of m[6]A-marked miRNAs in MDA-MB-231 cells (Figure 4A) as well as HEK293 cells (Figure S4). Moreover, the expression levels of these miRNAs were also dependent on METTL3 as their levels were similarly significantly reduced upon METTL3 depletion in both cell lines (Figures 4B and S4).

We next asked whether HNRNPA2B1 binds to pri-miRNA sites and whether it regulates the processing of METTL3/m[6]A dependent microRNAs. To answer these questions, we identified m[6]A peaks in pri-miRNA transcripts from m[6]A-seq data and searched for co-occurrence of HNRNPA2B1 binding sites. Consistent with a direct role for HNRNPA2B1 in regulating the processing of these pri-miRNA transcripts, we noted overlaps between m[6]A peaks and HNRNPA2B1 binding sites detected by HITS-CLIP (Figure 4C). Importantly, of the 61 miRNAs affected by HNRNPA2B1 depletion, 53 contained m[6]A-seq tags and 52 of those exhibited overlapping HNRNPA2B1 HITS-CLIP tags (p=3e-9, Figure 4D). These findings are consistent with recognition of the m[6]A mark by HNRNPA2B1 at miRNA loci.

If HNRNPA2B1 mediates its effects in the nucleus prior to the processing of pri-miRNAs to pre-miRNAs, then its depletion should result in the accumulation of pri-miRNA transcripts within the nucleus. Consistent with this, depletion of HNRNPA2B1 resulted in the accumulation of specific pri-miRNAs in the nucleus phenocopying the effect of METTL3 depletion (Figure 5A). HNRNPA2B1 thus positively regulates the nuclear processing of a set of pri-miRNAs. The processing of these pri-miRNAs is dependent on METTL3, the m[6]A writer, and HNRNPA2B1, a putative reader of this mark. These findings are consistent with a model wherein METTL3 and HNRNPA2B1 proteins comprise a pathway that controls the processing of a set of miRNA precursors.

A reader of m[6]A should serve as a bridge between this mark and effector proteins, or adaptor proteins that would ultimately interact with effectors. The effector involved in pri-miRNA processing is the Microprocessor complex, composed of the proteins DGCR8 and DROSHA. DGCR8 is an RNA-binding protein that recognizes the junction between the stem region and the flanking single-stranded RNA of the pri-miRNA hairpin. Hairpin recognition and binding allow for recruitment of the ribonuclease type III DROSHA, which cleaves the double stranded RNA to release the pre-miRNA molecule (Denli et al., 2004; Gregory et al., 2004; Han et al., 2004; Han et al., 2006; Landthaler et al., 2004). We had previously proposed the existence of one or more readers that could mediate the interaction between the m[6]A mark present in pri-miRNA regions and the Microprocessor to facilitate the recognition of the pri-miRNA among the large landscape of secondary structures that populate the transcriptome (Alarcon et al, 2015). Since HNRNPA2B1 recognizes m[6]A sequences and phenocopies the effects of METTL3, we investigated if it could link the m[6]A mark and the Microprocessor. Consistent with a direct role for HNRNPA2B1 in the regulation of pri-miRNA processing, immunoprecipitation of endogenous DGCR8 co-precipitated HNRNPA2B1, while reciprocal immunoprecipitation also revealed this interaction (Figure 5B–C). Importantly, this interaction persisted despite ribonuclease treatment, suggesting that the interaction between these two proteins is mediated by protein-protein interactions (Figure 5B–C). If HNRNPA2B1 recruits DGCR8 to a subset of pri-miRNA loci, then HNRNPA2B1 depletion should reduce the interaction of DGCR8 with pri-miRNA substrates. Consistent with this, HNRNPA2B1 depletion reduced the binding of endogenous DGCR8 with HNRNPA2B1-dependent pri-miRNA substrates (Figure 5D). HNRNPA2B1 thus recognizes m[6]A sequences, interacts with the Microprocessor, and facilitates the processing of a set of METTL3-dependent pri-miRNAs. These collective findings are consistent with its proposed role as a reader of the m[6]A mark.

HNRNPA2B1 binds methylated RNA

We next sought biochemical evidence for the *in vivo* interaction of HNRNPA2B1 with methylated RNA. MDA-MB-231 cells were UV-crosslinked, their nuclear fractions isolated, and endogenous HNRNPA2B1 was immunoprecipitated with a specific antibody. Upon HNRNPA2B1 immunoprecipitation and SDS-PAGE, immunoblotting with the m[6]A antibody revealed HNRNPA2B1 to interact with methylated RNA (Figure 6A). Importantly, ribonuclease treatment diminished the m6A signal of high molecular weight corresponding to long RNAs associated with HNRNPA2B1 but did not affect the m6A signal at the molecular weight of HNRNPA2B1 (37 kilodaltons) suggesting that HNRNPA2B1 directly associates with m[6]A methylated RNA and protects its RNA target sites from ribonuclease degradation (Figure 6A). The direct association between HNRNPA2B1 and m[6]A appears to be specific, since similar direct protection of m[6]A-containing RNA by another hnRNP RNA-binding protein was not observed (Figure S6A). If the methylated RNA that is bound by HNRNPA2B1 contains m[6]A, then depleting cells of the m[6]A writer METTL3 should reduce the HNRNPA2B1-bound m[6]A signal detected by western blot. Consistent with HNRNPA2B1 binding to cellular m[6]A, the m[6]A signal bound by endogenous HNRNPA2B1 recovered from METTL3 depleted cells was reduced relative to control cells (Figure 6B). Interestingly, Dominissini and colleagues used mass-spectrometry to identify candidate proteins that bound m[6]A modified RNA but not unmethylated RNA. Although not

functionally studied, HNRNPA2B1 was amongst the set of proteins identified that preferentially bound m^{6}A-modified RNA (Dominissini et al., 2012). Taken together, our findings reveal that endogenous HNRNPA2B1 directly interacts with m^{6}A-modified RNA *in vivo*.

We next studied the interaction between HNRNPA2B1 and methylated RNA *in vitro*. Purified full length HNRNPA2B1 exhibited some preference for binding methylated RNA probes relative to unmethylated ones as shown by gel shift assays (Figures S6B-C). The probes used for these assays correspond to sequences obtained from endogenous pri-miRNAs regions that contained m^{6}A-seq tags as well as endogenous HNRNPA2B1 binding sites (HITS-CLIP tags) (Figure S6D–E). Importantly, this preference was not observed using a different hnRNP protein (Figure S6F). We then generated a series of constructs containing GST-tagged individual domains. In isolation and under the conditions used in this study, only RRM1 exhibited a modest preference for m^{6}A-containing RNA (Figure S6G), however we cannot exclude the possibility that *in vivo* and in the context of full-length protein, additional protein domains could mediate or facilitate recognition and binding of the m^{6}A mark. These results suggest that HNRNPA2B1 can preferentially associate with m^{6}A-containing RNA *in vitro* and that the RRM1 motif could, in part, mediate this preference.

DISCUSSION

Our findings reveal that the HNRNPA2B1 RNA-binding protein binds the m^{6}A consensus motif and also directly binds the m^{6}A mark *in vivo* and *in vitro*. Loss-of-function experiments with HNRNPA2B1 and METTL3 resulted in similar effects on global alternative splicing patterns. HNRNPA2B1 was found to exhibit preferential *in vitro* binding to m^{6}A-modified RNA substrates used in this study over unmodified substrates. Additionally, HNRNPA2B1 interacts with the Microprocessor protein DGCR8, enhances binding of DGCR8 to pri-miRNA transcripts, and positively regulates pri-miRNA processing in a similar manner as METTL3, the m^{6}A writer. Moreover, we have identified a set of miRNAs whose processing is dependent on both METTL3 and HNRNPA2B1. These observations as a whole are consistent with a model wherein HNRNPA2B1 acts as a reader of the m^{6}A mark in the nucleus and mediates, in part, the effects of m^{6}A/METTL3 on microRNA processing (Figure 7).

YTHDF2 was recently identified as a cytoplasmic 'reader' protein of the m^{6}A mark. YTHDF2 was found to regulate the degradation of specific mRNAs by localizing them to processing bodies. The historical association of the m^{6}A mark with pre-mRNA processing (Carroll et al., 1990; Finkel and Groner, 1983; Katz et al., 2015; Stoltzfus and Dane, 1982) and the more recent molecular studies linking m^{6}A or components of the m^{6}A-methylation machinery with splicing (Dominissini et al., 2012; Granadino et al., 1990; Horiuchi et al., 2013; Little et al., 2000; Liu et al., 2014; Ortega et al., 2003; Ping et al., 2014; Schwartz et al., 2014; Wang et al., 2014b; Zhao et al., 2014) suggested the existence of a nuclear factor that could recognize this modification. Moreover, our recent work implicating m^{6}A/METTL3 in the processing of pri-miRNAs an event occurring in the nucleus also supported the existence of a nuclear 'reader' and effector of this mark (Alarcon et al., 2015). The role of HNRNPA2B1 in m^{6}A-dependent nuclear pri-miRNA processing and alternative splicing

events, its direct binding to m^{6}A and the RGAC motif *in vivo*, as well as its *in vitro* preference for specific m^{6}A-modified substrates relative to unmodified substrates support a role for this RNA-binding protein as a nuclear 'reader' and effector of this mark.

A natural question that arises is why there would exist distinct readers of m^{6}A that act within the nucleus or the cytoplasm? The fates of RNA molecules within the nucleus and cytoplasm are fundamentally distinct. Within the nucleus, nascent transcripts are internally processed to yield mature messages lacking introns. Similarly, primary microRNA transcripts are processed within the nucleus to yield shorter pre-miRNA forms the precursors for mature miRNAs. Within the cytoplasm, mRNAs can be localized to distinct compartments, translated, stabilized, or destabilized. The divergent processes in which transcripts participate in within the nucleus or cytoplasm are mediated by distinct protein complexes, such as the microRNA and splicing machineries in the nucleus or the deadenylation complex in the cytoplasm. The existence of distinct nuclear and cytoplasmic readers that bind m^{6}A but have additional protein-protein interaction domains would allow for each reader to interact with specific downstream effector proteins to mediate requisite events in the nucleus and cytoplasm. Consistent with this, YTHDF2 and HNRNPA2B1 contain distinct protein domains in addition to their RNA-binding domains P/Q/N-rich domain for YTHDF2 and RGG and M9 domains for HNRNPA2B1. These domains likely mediate interactions with specific cytoplasmic and nuclear effector proteins, respectively, or could form binding sites for adaptor proteins that recruit these machineries. In the case of HNRNPA2B1, its interaction with the Microprocessor represents an example of such selectivity. YTHDF2, on the other hand, has been shown to co-localize with components of the processing bodies in the cytoplasm (Wang et al., 2014a).

A long-standing question regarding m^{6}A has been the molecular basis for the localization of m^{6}A marks to specific infrequent (roughly one modification per 1000 bases) sites in transcripts (Rottman et al., 1994). The basis for this specificity is unknown, given that the m^{6}A consensus motif is short and therefore inherently non-specific. It has been proposed that local structural elements might contain the requisite contextual information that enables m^{6}A marks to be deposited (Rottman et al., 1994). Indeed, the methylation site in arguably the best-studied m^{6}A containing transcript (prolactin) falls in a predicted stem-loop/bulge structure (Rottman et al., 1994). Moreover, similar stem-loop/bulge structures were predicted for multiple m^{6}A consensus sites found in RSV RNA (Csepany et al., 1990; Kane and Beemon, 1985). With respect to 'writing' of this mark, METTL3 has been shown to methylate single-stranded RNA substrates *in vitro* to a similar degree as structured substrates (Liu et al., 2014). While others and we have identified many m^{6}A marks to also occur in regions that are not predicted to form structures, these historical findings suggest the presence of at least some m^{6}A marks in structured contexts. Future *in vivo* RNA structural mapping studies aimed at establishing the fraction of structured versus unstructured sites that contain the m^{6}A mark could provide important insights (Ding et al., 2014; Rouskin et al., 2014).

Another question that arises is whether the structured context within which m^{6}A occurs is important for its 'reading' by proteins such as HNRNPA2B1. While this question is beyond the scope of the current work and will require future genome-wide *in vivo* structural

analyses, we speculate that HNRNPA2B1 could potentially bind to m^{6}A at both unstructured/linear sites as well as in structured sites given its multiple RRM domains. At linear sites, the RRM1 domain could potentially bind m^{6}A-containing locations in linear RNA. At structured sites, the RRM1 domain could bind to an m^{6}A in a single-stranded loop of a stem-loop structure while the RRM2 domain could bind to a single-stranded bulge irrespective of m^{6}A-modification. Conversely, the RRM1 domain could bind an m^{6}A in the bulge of a stem-loop while the RRM2 domain could bind to a loop irrespective of its m^{6}A-modification. This speculative model is consistent with previously characterized transcriptome-wide binding of HNRNPA2B1 to AU-rich structural elements, which are less thermodynamically stable structures (Goodarzi et al., 2012). Another possibility is that the presence of the m^{6}A mark in double-stranded RNA could increase its open-conformation probability, thereby facilitating RRM1 binding to the m^{6}A-bearing strand (Roost et al., 2015). Thus, the presence of multiple RRM motifs in HNRNPA2B1 could enable it to bind cooperatively to two distinct sites such as a loop and a stem or a loop and a bulge within a stem-loop. Future structural and molecular studies are needed to shed light on the details and dynamics of the events that follow m^{6}A placement at linear and structured sites.

While we have implicated HNRNPA2B1, an RNA-binding protein implicated in several aspects of RNA biology (He and Smith, 2009; Villarroya-Beltri et al., 2013), as a downstream mediator of the effects of the m^{6}A mark/METTL3 in the nucleus, our findings do not exclude the possibility that there exist additional 'readers' of this mark within the nucleus that could mediate similar processing effects at other miRNA, exonic, or intronic loci or to mediate other aspects of RNA processing or localization. In fact, we have found that roughly half of the m^{6}A regulated miRNAs studied by us were dependent on HNRNPA2B1. This finding suggests the existence of additional nuclear 'readers' of this mark that mediate miRNA processing as well as other nuclear processing events. It would be quite interesting to determine whether other RNA-binding proteins of the hnRNP A/B family, that share similar RRM domains, recognize the m^{6}A modification and mediate, in part, its effects on nuclear processing events.

Our findings have identified HNRNPA2B1 as a nuclear 'reader', a downstream effector of the m^{6}A mark and an adaptor for the Microprocessor complex. Future proteomic and biochemical studies are needed to elucidate the molecular networks and mechanisms by which this reader mediates other nuclear processing events downstream of the m^{6}A mark.

EXPERIMENTAL PROCEDURES

Tissue culture

MDA-MB-231, HeLa, and HEK293T cell lines were purchased from ATCC. All cells were cultured *in vitro* in Dulbecco's modified Eagles medium (DMEM) supplemented with 10% fetal bovine serum (FBS), 1% penicillin-streptomycin, 2mM L-Glutamine, 1mM sodium pyruvate, and 2.5 ug/mL fungizone. All experiments were conducted with cells from passage 2 to 5.

Stable cell lines

Generation of lentivirus-mediated knockdowns was performed as described previously (Tavazoie et al., 2008). Commercially available shRNAs purchased from Sigma were co-transfected with lentivirus packaging plasmids in HEK293T cells to generate lentivirus. Two shRNAs targeting HNRNPA2B1 (TRCN0000001058, TRCN0000010582), two shRNAs specific for METTL3 (TRCN0000034715, TRCN0000034717), and a control shRNA (SHC002) were used for experiments. We generated stable fresh knock down cell-lines after 2 or 3 passages in order to avoid compensatory mechanisms of loss of knockdown.

qRT-PCR

Mature and pri-miRNAs were quantified by Taqman microRNA and Pri-miRNA assays. RNU44, U6 snRNA, GAPDH, and GusB were used as endogenous controls. Quantitative miRNAs expression data were obtained using the ABI Prism 7900HT Fast Real-Time PCR System and data was analyzed by Relative Quantification (RQ) Manager software.

Small RNA isolation

mirVana (Applied Biosystems) and Total RNA Purification Kit (Norgen Biotek) were used to extract total RNA from cells according to the manufacturer's instructions.

RNA sequencing

Samples were lysed using LB1 buffer (50 mM Hepes-KOH pH 7.5, 140 mM NaCl, 1 mM EDTA, 10% glycerol, 0.5% Triton x-100, and protease inhibitors). RNA was extracted from the nuclear fraction using the Total RNA Purification Kit (Norgen Biotek). RNA was subjected to RiboZero treatment (Epicentre), barcoded using ScriptSeq V2 kit (Epicentre) and sent for sequencing.

microRNA expression profiling (microarray)

The RNA extracted from two independent stable knockdowns of HNRNPA2B1 and two control cells expressing a control hairpin were labeled and hybridized on miRNA microarrays by LC sciences. Of all the probes included in the array, those corresponding to 329 miRNAs revealed a signal above background in at least two of the samples and were also expressed in the microarray previously performed using METTL3 depleted cells.

Supplementary Material

Refer to Web version on PubMed Central for supplementary material.

Acknowledgments

References

Alarcon CR, Lee H, Goodarzi H, Halberg N, Tavazoie SF. N6-methyladenosine marks primary microRNAs for processing. Nature. 2015; 519:482–485. [PubMed: 25799998]

Batista PJ, Molinie B, Wang J, Qu K, Zhang J, Li L, Bouley DM, Lujan E, Haddad B, Daneshvar K, et al. m(6)A RNA modification controls cell fate transition in mammalian embryonic stem cells. Cell stem cell. 2014; 15:707–719. [PubMed: 25456834]

Carroll SM, Narayan P, Rottman FM. N6-methyladenosine residues in an intron-specific region of prolactin pre-mRNA. Mol Cell Biol. 1990; 10:4456–4465. [PubMed: 2388614]

Csepany T, Lin A, Baldick CJ Jr, Beemon K. Sequence specificity of mRNA N6-adenosine methyltransferase. The Journal of biological chemistry. 1990; 265:20117–20122. [PubMed: 2173695]

Denli AM, Tops BB, Plasterk RH, Ketting RF, Hannon GJ. Processing of primary microRNAs by the Microprocessor complex. Nature. 2004; 432:231–235. [PubMed: 15531879]

Ding Y, Tang Y, Kwok CK, Zhang Y, Bevilacqua PC, Assmann SM. In vivo genome-wide profiling of RNA secondary structure reveals novel regulatory features. Nature. 2014; 505:696–700. [PubMed: 24270811]

Dominissini D, Moshitch-Moshkovitz S, Schwartz S, Salmon-Divon M, Ungar L, Osenberg S, Cesarkas K, Jacob-Hirsch J, Amariglio N, Kupiec M, et al. Topology of the human and mouse m6A RNA methylomes revealed by m6A-seq. Nature. 2012; 485:201–206. [PubMed: 22575960]

Elemento O, Slonim N, Tavazoie S. A universal framework for regulatory element discovery across all genomes and data types. Mol Cell. 2007; 28:337–350. [PubMed: 17964271]

Finkel D, Groner Y. Methylations of adenosine residues (m6A) in pre-mRNA are important for formation of late simian virus 40 mRNAs. Virology. 1983; 131:409–425. [PubMed: 6318439]

Giannopoulou EG, Elemento O. An integrated ChIP-seq analysis platform with customizable workflows. BMC Bioinformatics. 2011; 12:277. [PubMed: 21736739]

Goodarzi H, Najafabadi HS, Oikonomou P, Greco TM, Fish L, Salavati R, Cristea IM, Tavazoie S. Systematic discovery of structural elements governing stability of mammalian messenger RNAs. Nature. 2012; 485:264–268. [PubMed: 22495308]

Granadino B, Campuzano S, Sanchez L. The Drosophila melanogaster fl(2)d gene is needed for the female-specific splicing of Sex-lethal RNA. The EMBO journal. 1990; 9:2597–2602. [PubMed: 1695150]

Gregory RI, Yan KP, Amuthan G, Chendrimada T, Doratotaj B, Cooch N, Shiekhattar R. The Microprocessor complex mediates the genesis of microRNAs. Nature. 2004; 432:235–240. [PubMed: 15531877]

Hafner M, Landthaler M, Burger L, Khorshid M, Hausser J, Berninger P, Rothballer A, Ascano M, Jungkamp AC, Munschauer M, et al. PAR-CliP--a method to identify transcriptome-wide the binding sites of RNA binding proteins. Journal of visualized experiments : JoVE. 2010

Han J, Lee Y, Yeom KH, Kim YK, Jin H, Kim VN. The Drosha-DGCR8 complex in primary microRNA processing. Genes Dev. 2004; 18:3016–3027. [PubMed: 15574589]

Han J, Lee Y, Yeom KH, Nam JW, Heo I, Rhee JK, Sohn SY, Cho Y, Zhang BT, Kim VN. Molecular basis for the recognition of primary microRNAs by the Drosha-DGCR8 complex. Cell. 2006; 125:887–901. [PubMed: 16751099]

He Y, Smith R. Nuclear functions of heterogeneous nuclear ribonucleoproteins A/B. Cellular and molecular life sciences : CMLS. 2009; 66:1239–1256. [PubMed: 19099192]

Horiuchi K, Kawamura T, Iwanari H, Ohashi R, Naito M, Kodama T, Hamakubo T. Identification of Wilms' tumor 1-associating protein complex and its role in alternative splicing and the cell cycle. The Journal of biological chemistry. 2013; 288:33292–33302. [PubMed: 24100041]

Jaffrey SR. An expanding universe of mRNA modifications. Nature structural & molecular biology. 2014; 21:945–946.

Kane SE, Beemon K. Precise localization of m6A in Rous sarcoma virus RNA reveals clustering of methylation sites: implications for RNA processing. Mol Cell Biol. 1985; 5:2298–2306. [PubMed: 3016525]

Katz Y, Wang ET, Airoldi EM, Burge CB. Analysis and design of RNA sequencing experiments for identifying isoform regulation. Nat Methods. 2010; 7:1009–1015. [PubMed: 21057496]

Katz Y, Wang ET, Silterra J, Schwartz S, Wong B, Thorvaldsdottir H, Robinson JT, Mesirov JP, Airoldi EM, Burge CB. Quantitative visualization of alternative exon expression from RNA-seq data. Bioinformatics. 2015

Konig J, Zarnack K, Rot G, Curk T, Kayikci M, Zupan B, Turner DJ, Luscombe NM, Ule J. iCLIP reveals the function of hnRNP particles in splicing at individual nucleotide resolution. Nature structural & molecular biology. 2010; 17:909–915.

Landthaler M, Yalcin A, Tuschl T. The human DiGeorge syndrome critical region gene 8 and Its D. melanogaster homolog are required for miRNA biogenesis. Curr Biol. 2004; 14:2162–2167. [PubMed: 15589161]

Little NA, Hastie ND, Davies RC. Identification of WTAP, a novel Wilms' tumour 1-associating protein. Human molecular genetics. 2000; 9:2231–2239. [PubMed: 11001926]

Liu J, Yue Y, Han D, Wang X, Fu Y, Zhang L, Jia G, Yu M, Lu Z, Deng X, et al. A METTL3-METTL14 complex mediates mammalian nuclear RNA N6-adenosine methylation. Nature chemical biology. 2014; 10:93–95. [PubMed: 24316715]

Liu N, Dai Q, Zheng G, He C, Parisien M, Pan T. N(6)-methyladenosine-dependent RNA structural switches regulate RNA-protein interactions. Nature. 2015; 518:560–564. [PubMed: 25719671]

Meyer KD, Saletore Y, Zumbo P, Elemento O, Mason CE, Jaffrey SR. Comprehensive analysis of mRNA methylation reveals enrichment in 3′ UTRs and near stop codons. Cell. 2012; 149:1635–1646. [PubMed: 22608085]

Ortega A, Niksic M, Bachi A, Wilm M, Sanchez L, Hastie N, Valcarcel J. Biochemical function of female-lethal (2)D/Wilms' tumor suppressor-1-associated proteins in alternative pre-mRNA splicing. The Journal of biological chemistry. 2003; 278:3040–3047. [PubMed: 12444081]

Ping XL, Sun BF, Wang L, Xiao W, Yang X, Wang WJ, Adhikari S, Shi Y, Lv Y, Chen YS, et al. Mammalian WTAP is a regulatory subunit of the RNA N6-methyladenosine methyltransferase. Cell research. 2014; 24:177–189. [PubMed: 24407421]

Roost C, Lynch SR, Batista PJ, Qu K, Chang HY, Kool ET. Structure and thermodynamics of N6-methyladenosine in RNA: a spring-loaded base modification. Journal of the American Chemical Society. 2015; 137:2107–2115. [PubMed: 25611135]

Rottman FM, Bokar JA, Narayan P, Shambaugh ME, Ludwiczak R. N6-adenosine methylation in mRNA: substrate specificity and enzyme complexity. Biochimie. 1994; 76:1109–1114. [PubMed: 7748945]

Rouskin S, Zubradt M, Washietl S, Kellis M, Weissman JS. Genome-wide probing of RNA structure reveals active unfolding of mRNA structures in vivo. Nature. 2014; 505:701–705. [PubMed: 24336214]

Schibler U, Kelley DE, Perry RP. Comparison of methylated sequences in messenger RNA and heterogeneous nuclear RNA from mouse L cells. Journal of molecular biology. 1977; 115:695–714. [PubMed: 592376]

Schwartz S, Mumbach MR, Jovanovic M, Wang T, Maciag K, Bushkin GG, Mertins P, Ter-Ovanesyan D, Habib N, Cacchiarelli D, et al. Perturbation of m6A writers reveals two distinct classes of mRNA methylation at internal and 5′ sites. Cell reports. 2014; 8:284–296. [PubMed: 24981863]

Stoltzfus CM, Dane RW. Accumulation of spliced avian retrovirus mRNA is inhibited in S-adenosylmethionine-depleted chicken embryo fibroblasts. Journal of virology. 1982; 42:918–931. [PubMed: 6285005]

Tavazoie SF, Alarcon C, Oskarsson T, Padua D, Wang Q, Bos PD, Gerald WL, Massague J. Endogenous human microRNAs that suppress breast cancer metastasis. Nature. 2008; 451:147–152. [PubMed: 18185580]

Ule J, Jensen K, Mele A, Darnell RB. CLIP: a method for identifying protein-RNA interaction sites in living cells. Methods. 2005; 37:376–386. [PubMed: 16314267]

Villarroya-Beltri C, Gutierrez-Vazquez C, Sanchez-Cabo F, Perez-Hernandez D, Vazquez J, Martin-Cofreces N, Martinez-Herrera DJ, Pascual-Montano A, Mittelbrunn M, Sanchez-Madrid F.

Sumoylated hnRNPA2B1 controls the sorting of miRNAs into exosomes through binding to specific motifs. Nature communications. 2013; 4:2980.

Wang X, Lu Z, Gomez A, Hon GC, Yue Y, Han D, Fu Y, Parisien M, Dai Q, Jia G, et al. N6-methyladenosine-dependent regulation of messenger RNA stability. Nature. 2014a; 505:117–120. [PubMed: 24284625]

Wang Y, Li Y, Toth JI, Petroski MD, Zhang Z, Zhao JC. N(6)-methyladenosine modification destabilizes developmental regulators in embryonic stem cells. Nat Cell Biol. 2014b; 16:191–198. [PubMed: 24394384]

Wei CM, Moss B. Methylation of newly synthesized viral messenger RNA by an enzyme in vaccinia virus. Proc Natl Acad Sci U S A. 1974; 71:3014–3018. [PubMed: 4606808]

Zhang C, Darnell RB. Mapping in vivo protein-RNA interactions at single-nucleotide resolution from HITS-CLIP data. Nat Biotechnol. 2011; 29:607–614. [PubMed: 21633356]

Zhao X, Yang Y, Sun BF, Shi Y, Yang X, Xiao W, Hao YJ, Ping XL, Chen YS, Wang WJ, et al. FTO-dependent demethylation of N6-methyladenosine regulates mRNA splicing and is required for adipogenesis. Cell research. 2014; 24:1403–1419. [PubMed: 25412662]

RESEARCH HIGHLIGHTS

- HNRNPA2B1 binds m^{6}A containing sites and RGAC motif in nuclear transcripts

- HNRNPA2B1 mediates m^{6}A-dependent primary-microRNA processing events

- HNRNPA2B1 modulation causes similar effects on alternative splicing as METTL3 modulation

Author Manuscript

Author Manuscript

Author Manuscript

Author Manuscript
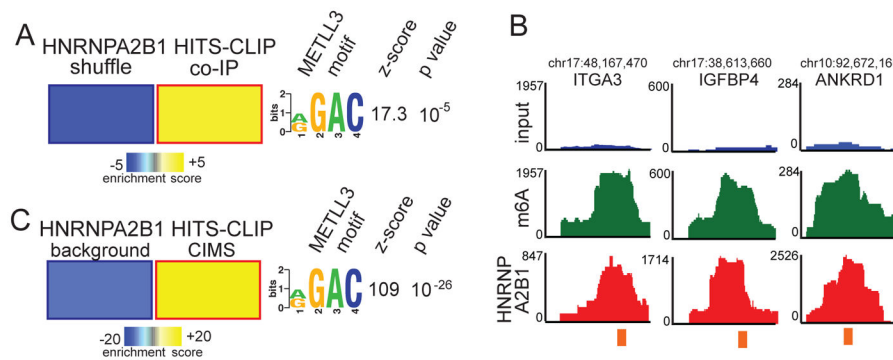
Figure 1. HNRNPA2B1 recognizes m⁶A methylated sequences

(A) FIRE, in non-discovery mode, was used to assess enrichment of the RGAC motif among the HNRNPA2B1 HITS-CLIP peaks, obtained from MDA-MB-231 cells, relative to randomly generated sequences with similar dinucleotide frequencies. The figure shows a significant enrichment of the m⁶A motif (RGAC) in HNRNPA2B1 binding sites, where yellow indicates over-representation and blue represents under-representation. The magnitude of the representation is as per the heat-map scale shown at the bottom. The associated *z*-score and *p*-value are also provided.

(B) RNA sequencing read density at exemplary loci where HNRNPA2B1 and m⁶A peaks intersect. Shown are the input nuclear RNA (blue), m⁶A-seq (green), and HNRNPA2B1 HITS-CLIP (red) reads. The orange bar denotes the sequence match to the RGAC motif.

(C) FIRE analysis of the enrichment of the RGAC motif in the HNRNPA2B1 footprints. Sequences within 5nt of HNRNPA2B1 cross-linking induced deletions generated by HITS-CLIP protocol were significantly enriched for the RGAC motif when compared to background deletions. The motif, *p*-value and *z*-score are also shown.
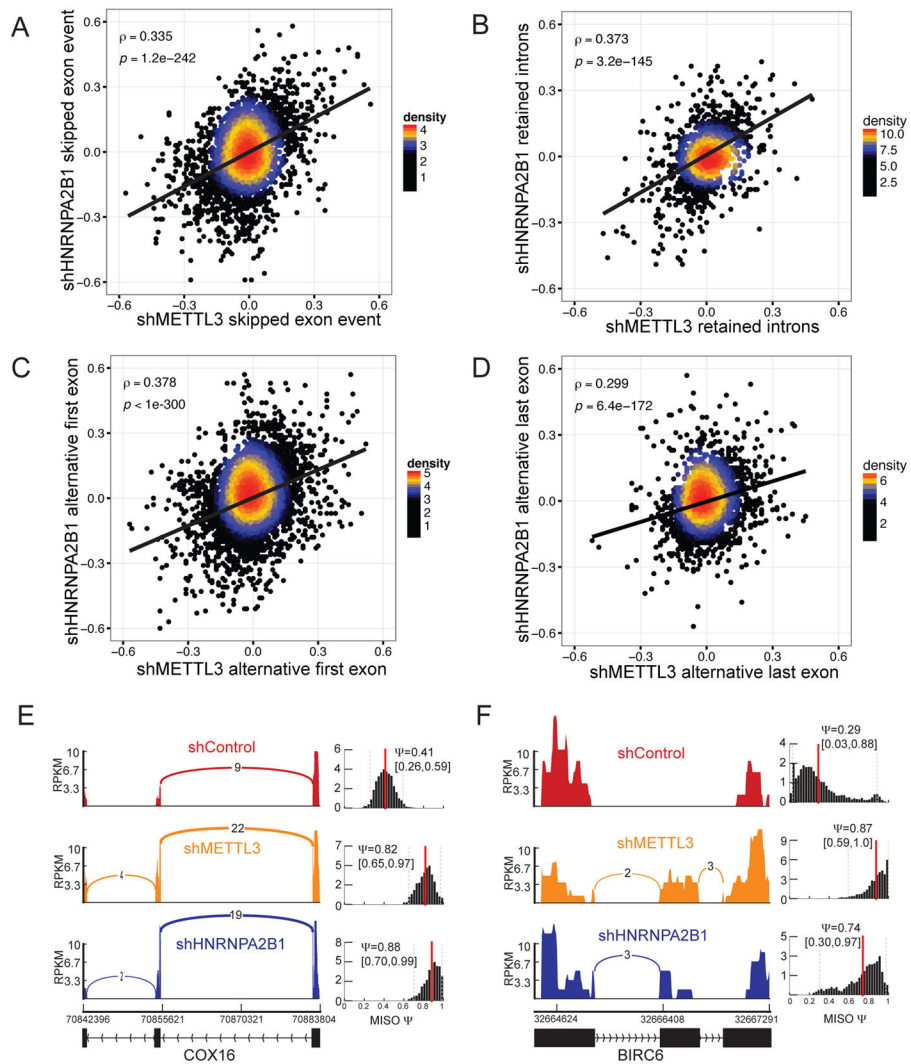
Figure 2. Depletion of HNRNPA2B1 and METTL3 similarly affect RNA splicing

(A–D) Correlation between differential percent spliced in (ψ) in annotated alternative splicing events following HNRNPA2B1 and METLL3 depletion. Annotated skipped exons (A), retained introns (B), alternative first exons (C), and alternative last exons (D) were quantified in HNRNPA2B1 and METTL3 knockdown MDA-MB-231 cells respectively (relative to control cells). Spearman correlation was then used to assess the similarity in splicing modulations following depletion of METTL3 (m[6]A writer) and HNRNPA2B1 (m[6]A reader).

(E) Exemplary sashimi plots (Katz et al., 2015) showing concerted alternative splicing changes that occurred in MDA-MB-231 cells depleted of METTL3 or HNRNPA2B1.

(F) Exemplary of sashimi plots as in E but using an independent cell line, HeLa. Shown are the normalized coverage at each exon, along with the estimated ψ value (percent spliced in). For example, in this case, 29% of transcripts were estimated to contain the skipped exon in the control sample, while this estimate was increased to 87% and 74% for METTL3 and HNRNPA2B1 depleted cells, respectively.
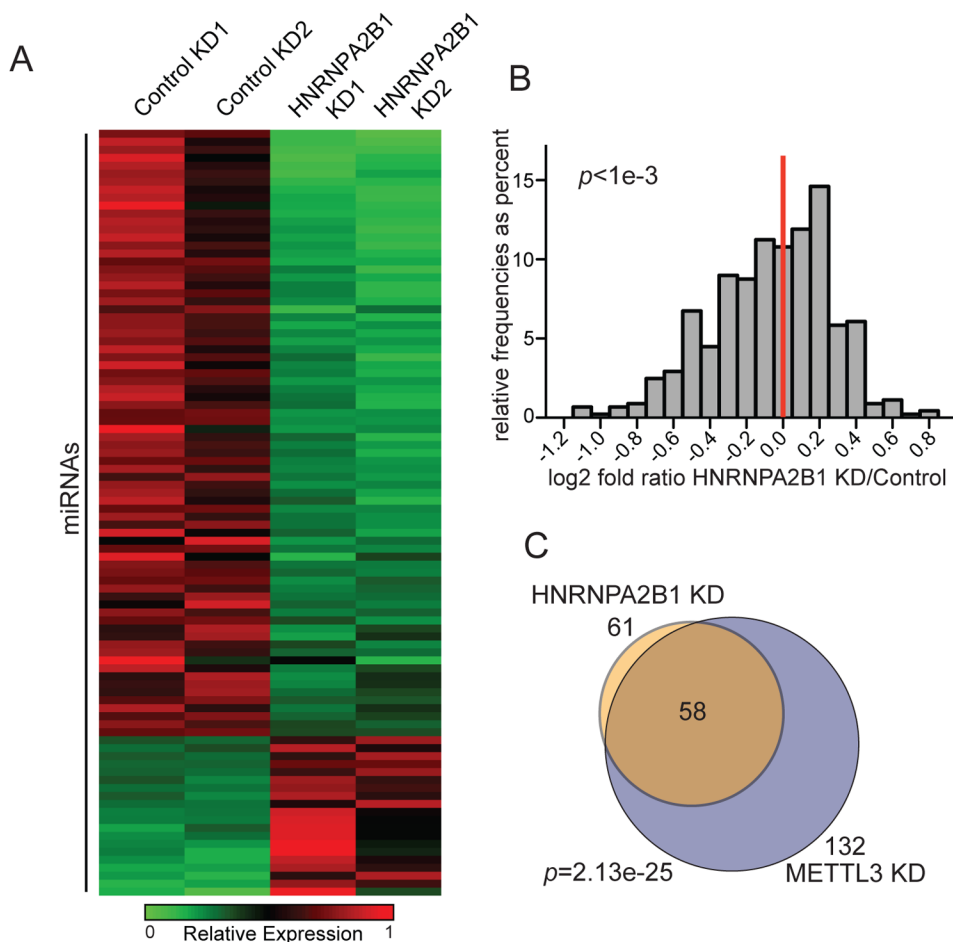
Figure 3. Depletion of HNRNPA2B1 impacts miRNA production

(A) Heat map depicting the miRNAs affected at least by 50% by 2 independent shRNAs targeting HNRNPA2B1 in HEK293 cells. Red represents higher expression and green lower expression levels.

(B) Histogram of the fold change (log$_2$) observed in miRNA expression, as obtained by genome-wide miRNA expression profiling shown in (A). The ratio of the average level for the two independent shRNAs over the average of the two controls is shown. The p-value of the two-sample Kolmogorov-Smirnov test is indicated.

(C) Venn diagram depicting the intersection of miRNAs that were reduced by greater than 50% upon HNRNPA2B1 or METTL3 depletion. 132 miRNAs were downregulated by more than 50% upon METTL3 depletion and 61 miRNAs were downregulated by 50% upon HNRNPA2B1 depletion. The extent of miRNAs detected by microarray in both experiments was 329. The p-value was calculated based on the hypergeometric distribution.
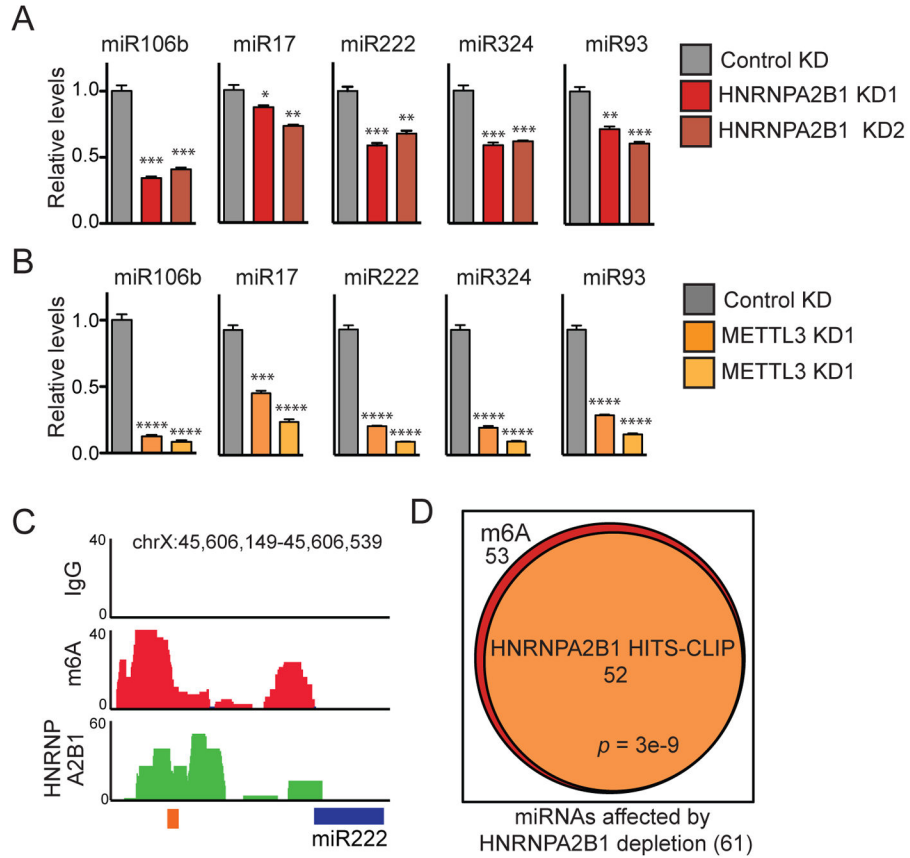
Figure 4. HNRNPA2B1 binds to m⁶A-methylated pri-miRNA sequences

(A) qRT-PCR quantification of exemplary miRNAs that were modulated by HNRNPA2B1 depletion in MDA-MB-231 cells. Stable cell lines expressing shControl vector or two independent shRNAs targeting HNRNPA2B1 were generated and total RNA was extracted and quantified. ***, *p*-value <1E-3; **, *p*-value <1E-2; *, *p*-value <5E-2.

(B) Quantification of the expression levels of miRNAs shown in (A) when METTL3 was depleted in MDA-MB-231 cells by 2 independent shRNAs, as measured by qRT-PCR. *P*-values as in (A). ****, *p*-value <5E-4; ***, *p*-value <1E-3.

(C) Genome tracks depicting sequencing read coverage from m⁶A-seq (red) and HNRNPA2B1 HITS-CLIP (green) within an exemplary pri-miRNA obtained from MDA-MB-231 cells. The upper track represents the reads from the IgG immunoprecipitated control sample. The blue box indicates the position of the pre-miRNA and the orange box indicates the position of the RGAC motif. The chromosomal location of the sequence depicted in the figure is shown at the top of the panel.

(D) Venn diagram showing the overlap between m⁶A-seq tags and HNRNPA2B1-HITS-CLIP tags within pri-miRNA regions of miRNAs affected by HNRNPA2B1 depletion. The *p*-value was calculated based on the hypergeometric distribution.
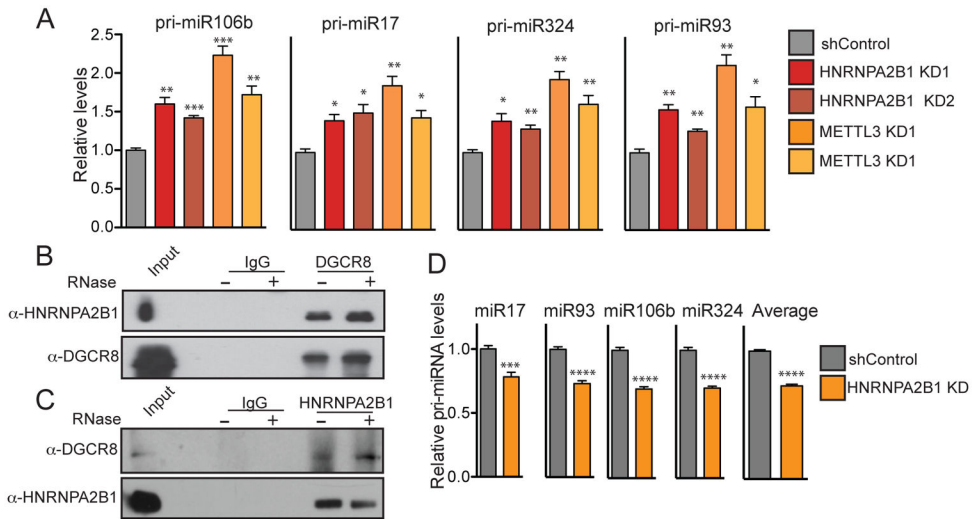
Figure 5. HNRNPA2B1 regulates miRNA processing and interacts with the Microprocessor

(A) Pri-miRNA expression levels for the miRNAs shown in (4B–C) upon HNRNPA2B1 and METTL3 depletion as measured by qRT-PCR. All experiments were performed in biological triplicates. ***, p-value <1E-3; **, p-value <1E-2; *, p-value <5E-2.

(B) *In vivo* interaction between DGCR8 and HNRNPA2B1. HEK293 cells were chemically crosslinked before antibody-mediated immunoprecipitation of endogenous DGCR8. After immunoprecipitation, samples were washed and incubated with RNAse as indicated. Western blots for HNRNPA2B1 and DGCR8 are shown.

(C) Same as B, but the reciprocal immunoprecipitation was performed. In this case endogenous HNRNPA2B1 was immunoprecipitated and its interaction with DGCR8 was detected by Western blot under similar conditions.

(D) Quantification of DGCR8-bound pri-miRNAs. Endogenous DGCR8 was immunoprecititated after UV-crosslinking and pri-miRNAs bound to it were extracted and quantified by qRT-PCR. The bar graph shows the qRT-PCR of a panel of HNRNPA2B1-target miRNAs for which expression was shown to be reduced upon HNRNPA2B1 depletion. ****, p-value <5E-4; ***, p value-<1E-3.
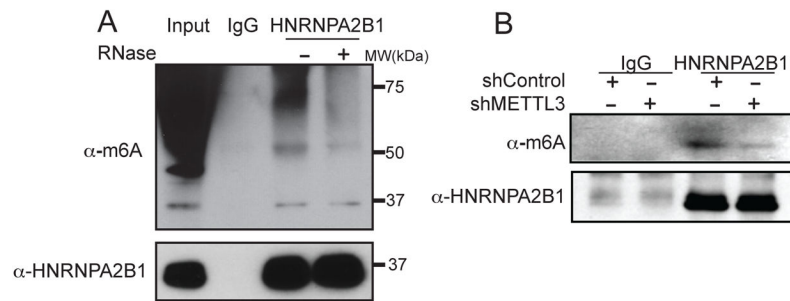
Figure 6. HNRNPA2B1 binds m^6A methylated RNA

(A) Immunoprecipitation of endogenous HNRNPA2B1 from MDA-MB-231 cells. Cells were UV-crosslinked before immunoprecipitation and samples were treated with RNase-A or left untreated as indicated after the immunoprecipitation. Western blotting was performed using the indicated antibodies.

(B) Immunoprecipitation of endogenous HNRNPA2B1 and associated RNA from control cells or cells depleted of METTL3. Cells were UV-crosslinked prior to immunoprecipitation and Western blotting was done using the antibodies depicted in the figure.
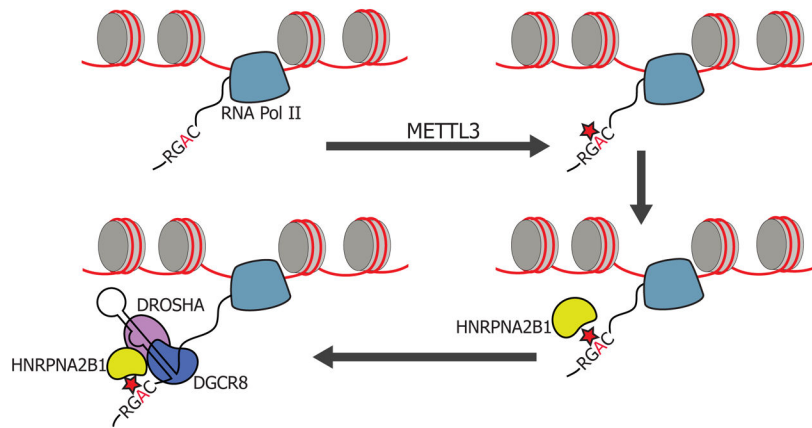
Figure 7. HNRNPA2B1 is a mediator of the m⁶A mark

Schematic representation of the nuclear role of HNRNPA2B1 in miRNA processing. HNRNPA2B1 is shown as a reader of the m⁶A methylation mark. Pri-miRNA processing is depicted in the model. The red star represents m⁶A mark on RNA; and the yellow shape represents the HNRNPA2B1 RNA-binding protein. A similar model could be use to depict alternative splicing, in which HNRNPA2B1 binding to m⁶A methylated pre-mRNAs would facilitate the engagement of splicing factors.